Published for SISSA by Springer
Received: June 5, 2023
Accepted: September 5, 2023
Published: September 13, 2023

Thermal leptogenesis in the minimal gauged $U(1)_{L_\mu - L_\tau}$ model

A. Granelli,[a,b] **K. Hamaguchi,**[c,d] **N. Nagata,**[c] **M.E. Ramirez-Quezada**[c,e] **and J. Wada**[c]

[a] *Dipartimento di Fisica e Astronomia, Università di Bologna, via Irnerio 46, 40126 Bologna, Italy*
[b] *INFN, Sezione di Bologna, viale Berti Pichat 6/2, 40127 Bologna, Italy*
[c] *Department of Physics, University of Tokyo, Bunkyo-ku, Tokyo 113-0033, Japan*
[d] *Kavli Institute for the Physics and Mathematics of the Universe (Kavli IPMU), University of Tokyo, Kashiwa 277-8583, Japan*
[e] *Dual CP Institute of High Energy Physics, C.P. 28045, Colima, Mexico*

E-mail: alessandro.granelli@unibo.it, hama@hep-th.phys.s.u-tokyo.ac.jp, natsumi@hep-th.phys.s.u-tokyo.ac.jp, me.quezada@hep-th.phys.s.u-tokyo.ac.jp, wada@hep-th.phys.s.u-tokyo.ac.jp

Abstract: We discuss the thermal leptogenesis mechanism within the minimal gauged $U(1)_{L_\mu - L_\tau}$ model to explain the observed baryon asymmetry of the Universe (BAU). In such framework, the phases of the Pontecorvo-Maki-Nakagawa-Sakata neutrino mixing matrix and the sum of the Standard Model neutrino masses are predictable because of a restricted neutrino mass matrix structure. Additionally, in the context of thermal leptogenesis, the BAU can be computed in terms of the three remaining free variables that parameterise the right-handed neutrino masses and their Yukawa couplings to the Higgs and lepton doublets. We identify the ranges of such parameters for which the correct BAU can be reproduced. We adopt the formalism of the density matrix equations to fully account for flavour effects and consider the decays of all the three right-handed neutrinos. Our analysis reveals that thermal leptogenesis is feasible within a wide parameter space, specifically for Yukawa couplings ranging from approximate unity to $\mathcal{O}(0.03\text{–}0.05)$ and mass of the lightest right-handed neutrino $M_1 \gtrsim 10^{11-12}\,\mathrm{GeV}$, setting a leptogenesis scale in the considered model which is higher than that of the non-thermal scenario.

Keywords: Baryo-and Leptogenesis, Cosmology of Theories BSM, Baryon/Lepton Number Violation

ArXiv ePrint: 2305.18100

https://doi.org/10.1007/JHEP09(2023)079

JHEP09(2023)079

Contents

JHEP09(2023)079

1 Introduction

There is astrophysical and cosmological evidence for the existence of a matter-antimatter asymmetry in the present Universe. The baryon-to-photon ratio parameterises the baryon asymmetry of the Universe (BAU),

$$\eta_B = \frac{n_B - n_{\bar{B}}}{n_\gamma}, \tag{1.1}$$

where n_B, $n_{\bar{B}}$, and n_γ are the number densities of baryons, anti-baryons, and photons, respectively. The baryon-to-photon ratio has been determined independently from observations of the Cosmic Microwave Background (CMB) anisotropies and Big Bang Nucleosynthesis (BBN) estimates. Both estimations are consistent with the best-fit value $\eta_B \simeq 6.1 \times 10^{-10}$ [1, 2]. One compelling mechanism that explains the observed BAU is leptogenesis [3] based on the existence of right-handed neutrinos and their out-of-equilibrium decays in the early Universe. In the simplest thermal leptogenesis scenario, the CP-violating, out-of-equilibrium decays of the right-handed neutrinos generate a lepton asymmetry, which is converted into a baryon asymmetry by the sphaleron processes predicted by the SM [4]. The leptogenesis mechanism for the BAU generation can be studied in a wide range of models beyond the SM, providing a valuable window into the study of new physics (see, e.g., ref. [5] for a recent review on the topic and references therein).

In this paper, we focus on a model that exhibits a novel anomaly-free U(1) gauge symmetry denoted by $U(1)_{L_\mu - L_\tau}$ [6–9], where L_e, L_μ and L_τ stand for the lepton number (flavour) associated to the electron (e), muon (μ) and tauon (τ), respectively. The model is implemented within the framework of the type-I seesaw mechanism [10–14], hence providing an explanation for the smallness of SM neutrino masses through the introduction of three

heavy right-handed neutrinos $N_{1,2,3}$ with masses $M_{1,2,3}$. The symmetry of the model imposes constraints on the neutrino mass structure, since the second and third-generation leptons, μ and τ, are charged under $\mathrm{U}(1)_{L_\mu - L_\tau}$ while the electron is not. Consequently, the Dirac mass matrix has a simple diagonal structure, and only certain components of the Majorana matrix are non-zero. This simple mass structure is insufficient to explain neutrino oscillation data [15, 16], and hence, the $\mathrm{U}(1)_{L_\mu - L_\tau}$ must be broken. This is typically achieved by introducing a scalar field that has non-zero $\mathrm{U}(1)_{L_\mu - L_\tau}$ charge and a vacuum expectation value (VEV), which breaks the gauge symmetry giving mass to the $\mathrm{U}(1)_{L_\mu - L_\tau}$ gauge bosons. We refer to this model as the "minimal gauged $\mathrm{U}(1)_{L_\mu - L_\tau}$ model". The model has a strong predictive power [15–24] because of the so-called two-zero minor structure [17–19, 21–23] of the neutrino mass matrix.

The aim of the present work is to study thermal leptogenesis in the minimal gauged $\mathrm{U}(1)_{L_\mu - L_\tau}$ model.[1] Since the neutrino mass structure is highly restricted in the model, it is not obvious whether the observed BAU is obtainable through thermal leptogenesis. In a widely-considered setup for thermal leptogenesis [28], the right-handed neutrinos mass spectrum is strongly hierarchical, $M_1 \ll M_2 \ll M_3$, and the lepton asymmetries in the three flavours evolve equally. This scenario has been extensively studied solving the unflavoured Boltzmann Equations (BEs) and is subject to a model-independent bound on the mass scale of leptogenesis, reading $M_1 \gtrsim 10^9$ GeV, below which the requisite CP-asymmetry is too small to get the observed value of the BAU [29–33]. However, in our model, the condition of a strong mass hierarchy is not satisfied in many parts of the parameter space, and we expect the decay of each of the three right-handed neutrinos to contribute to the generation of the BAU.

Charged lepton flavour effects can also play a crucial role in the generation of the BAU [34–43]. Specifically, the unflavoured scenario is valid only in the single-flavour regime for temperatures above $\sim 10^{12}$ GeV, when the processes mediated by the charged lepton SM Yukawa couplings are out-of-equilibrium. In the two-flavour regime $10^9 \ll T/\mathrm{GeV} \ll 10^{12}$, processes induced by the τ-Yukawa coupling occur at a rate Γ_τ much larger than the Hubble expansion rate H, which indicates that these processes are in thermal equilibrium. Consequently, the asymmetries in the lepton charge L_τ and $L_\mu + L_e$ evolve differently in this regime. Similarly, in the three-flavour regime for $T \ll 10^9$ GeV, processes mediated by the μ-Yukawa coupling with rate Γ_μ are also in thermal equilibrium ($\Gamma_\mu \gg H$), leading to the individual evolution of L_e, L_μ and L_τ. Given that the mass scales of interest cover different flavour regimes, the simplest unflavoured scenario is not applicable to our study, and we have to consider the impact of charged lepton flavour effects on the BAU generation.

The study of thermal leptogenesis in the (three-) two-flavour regime can be conducted using the formalism of (three-) two-flavoured BEs, provided that the processes mediated by the (μ- and τ-) τ-Yukawa couplings are sufficiently fast. In this formalism, the equations for the asymmetries in (L_τ, L_μ and L_e) L_τ and $L_\mu + L_e$ are different and solved separately. However, to accurately account for flavour effects, it is more precise to trace the evolution of the elements of the density matrix of the lepton flavour system with the Density Matrix

[1] For a study of the non-thermal leptogenesis mechanism within the minimal gauged $\mathrm{U}(1)_{L_\mu - L_\tau}$ model, see ref. [24]. Leptogenesis in (non-minimal) gauged $\mathrm{U}(1)_{L_\mu - L_\tau}$ models is also discussed in refs. [25–27].

JHEP09(2023)079

Equations (DMEs) [40–43]. This approach is particularly useful when the processes mediated by the charged lepton Yukawa couplings are neither infinitely fast nor their effects negligible, such as at the transitions between different flavour regimes, and has been shown to lead to different predictions with respect to the BEs [40–45].

The presence of multiple decaying right-handed neutrinos also has implications for the generation of the BAU, specifically because of the effects of heavy neutrino flavours. The right-handed neutrinos couple to different superpositions of flavour states, whose interactions can induce additional decoherence effects in the context of the DMEs [42] (see also ref. [43]). These effects can be particularly relevant when the right-handed neutrinos do not have a strongly hierarchical mass spectrum, which is the case in certain parts of the parameter space of the considered model where $M_2 \lesssim 3M_1$ and $M_3 \lesssim 3M_2$. In this regime, the different superposition of flavour states, associated with the different right-handed neutrinos, are simultaneously present in the Universe.

In this work, we consider the formalism of the DMEs with three decaying right-handed neutrinos to fully account for all the relevant effects mentioned above. By performing a numerical scan of the parameter space, we investigate for which values of the parameters of the minimal gauge $\mathrm{U}(1)_{L_\mu - L_\tau}$ model the DMEs are successful in reproducing the observed BAU. We solve numerically the DMEs for thermal leptogenesis using the Python package `ULYSSES` [46, 47], that is a freely accessible code for the numerical evaluation of the BAU in the context of leptogenesis. Its major features are the variety of equations available, allowing for comparisons between the BEs and DMEs in the different regimes, and a rapid evaluation, making scans of large parameter spaces feasible over relatively short periods of time.

The paper is structured as follows. In section 2, we present the minimal gauged $\mathrm{U}(1)_{L_\mu - L_\tau}$ model and analyse the corresponding neutrino mass structure. In section 3, we discuss in more details the mechanism of thermal leptogenesis and the formalism of DMEs. We introduce the DMEs with three decaying right-handed neutrinos and the corresponding CP-asymmetry parameters, which are crucial for understanding the generation of the lepton and baryon asymmetries in the early Universe. The results of the scan of the parameter space for viable leptogenesis is presented in section 4, and we finally conclude in section 5.

2 The minimal gauged $\mathrm{U}(1)_{L_\mu - L_\tau}$ model

In the minimal gauged $\mathrm{U}(1)_{L_\mu - L_\tau}$ model, the second and third-generation leptons, namely those of lepton flavour μ and τ, carry charges of $+1$ and -1, respectively. Notably, the first-generation leptons (of lepton flavour e), quarks, and the Higgs field in the Standard Model (SM) are not charged under this particular gauge symmetry. Moreover, we introduce three right-handed sterile neutrinos, N_e, N_μ, and N_τ, each described by a Weyl spinor that transforms under the $(0, \frac{1}{2})$ representation of the Lorentz group (thus right-handed), which are singlets under the SM gauge group (thus sterile) and carry the $\mathrm{U}(1)_{L_\mu - L_\tau}$ charges 0, $+1$, and -1, respectively. Additionally, we introduce a scalar boson σ, which is a singlet under the SM gauge group and carries the $\mathrm{U}(1)_{L_\mu - L_\tau}$ charge $+1$. This scalar field develops a VEV that spontaneously breaks the $\mathrm{U}(1)_{L_\mu - L_\tau}$ gauge symmetry. We summarise the charges of the field content of this model in table 1, denoting the left-handed SU(2) lepton doublets of

JHEP09(2023)079

$L_\mu - L_\tau$ Charges of the Field Content					
	ℓ_e, e_R, N_e	ℓ_μ, μ_R, N_μ	$\ell_\tau, \tau_R, N_\tau$	σ	Others
$L_\mu - L_\tau$	0	+1	−1	+1	0

Table 1. The $L_\mu - L_\tau$ charges of the field content in the considered minimal gauged $\mathrm{U}(1)_{L_\mu - L_\tau}$ model.

flavour α with ℓ_α and the right-handed charged leptons with α_R, $\alpha = e,\ \mu,\ \tau$. We adopt a two-component spinor notation (see, e.g., ref. [48]) as in ref. [21].

For the purposes of our discussion, we focus on the new leptonic interactions involving the right-handed neutrinos and their Majorana mass terms, reading

$$\begin{aligned}\Delta\mathcal{L} = &-\lambda_e N_e^c(\ell_e\cdot\Phi) - \lambda_\mu N_\mu^c(\ell_\mu\cdot\Phi) - \lambda_\tau N_\tau^c(\ell_\tau\cdot\Phi)\\ &-\frac{1}{2}M_{ee}N_e^cN_e^c - M_{\mu\tau}N_\mu^cN_\tau^c - \lambda_{e\mu}\sigma N_e^cN_\mu^c - \lambda_{e\tau}\sigma^* N_e^cN_\tau^c + \text{h.c.}\,,\end{aligned} \tag{2.1}$$

where the dots indicate the contraction of the SU(2) indices between the lepton doublets and the Higgs doublet Φ. Additionally, $(N_\alpha^c)_a \equiv \varepsilon_{ab}(N_\alpha^*)_b$, where $\alpha = e,\ \mu,\ \tau$ and ε_{ab} is the antisymmetric tensor of the spinor indices a, b. The interaction terms in eq. (2.1) lead to neutrino mass terms after the Higgs field Φ and singlet scalar σ acquire their VEVs, denoted as $\langle\Phi\rangle = v/\sqrt{2}$ and $\langle\sigma\rangle$, respectively. These mass terms can be expressed as follows:

$$\mathcal{L}_{\text{mass}} = -(\nu_e,\nu_\mu,\nu_\tau)\mathcal{M}_D\begin{pmatrix}N_e^c\\N_\mu^c\\N_\tau^c\end{pmatrix} - \frac{1}{2}(N_e^c,N_\mu^c,N_\tau^c)\mathcal{M}_R\begin{pmatrix}N_e^c\\N_\mu^c\\N_\tau^c\end{pmatrix} + \text{h.c.}\,, \tag{2.2}$$

where ν_α, are the left-handed Weyl spinors describing the SM neutrinos of lepton flavour α, $\mathcal{M}_D$ is the Dirac mass matrix and $\mathcal{M}_R$ is the Majorana mass matrix given by,

$$\mathcal{M}_D = \frac{v}{\sqrt{2}}\begin{pmatrix}\lambda_e & 0 & 0\\ 0 & \lambda_\mu & 0\\ 0 & 0 & \lambda_\tau\end{pmatrix}, \qquad \mathcal{M}_R = \begin{pmatrix}M_{ee} & \lambda_{e\mu}\langle\sigma\rangle & \lambda_{e\tau}\langle\sigma\rangle\\ \lambda_{e\mu}\langle\sigma\rangle & 0 & M_{\mu\tau}\\ \lambda_{e\tau}\langle\sigma\rangle & M_{\mu\tau} & 0\end{pmatrix}, \tag{2.3}$$

respectively. Notably the Dirac mass matrix $\mathcal{M}_D$ is diagonal, while the (μ,μ) and (τ,τ) components in the Majorana mass matrix $\mathcal{M}_R$ are zero due to the $\mathrm{U}(1)_{L_\mu - L_\tau}$ gauge symmetry. This particular structure leads to interesting predictions for neutrino observables [19, 21, 22, 49, 50], as discussed below. For the remainder of this discussion, we assume that the Dirac Yukawa couplings λ_e, λ_μ, and λ_τ, as well as the VEVs v and $\langle\sigma\rangle$ are real without loss of generality, with $v = 246\,\text{GeV}$; this can always be realised via field redefinition.

The seesaw master formula can naturally explain the smallness of SM neutrino masses by assuming that the non-zero components in the Majorana mass matrix are much larger than those in the Dirac matrix. The formula relates the light neutrino masses to the masses of the heavy right-handed neutrinos, and their couplings to the SM particles [10–14],

$$\mathcal{M}_{\nu_L} \simeq -\mathcal{M}_D\mathcal{M}_R^{-1}\mathcal{M}_D^T\,. \tag{2.4}$$

JHEP09(2023)079

The mass matrix can be diagonalised, allowing us to express the flavour eigenstates of the neutrinos as linear combinations of the mass eigenstates,

$$U^T \mathcal{M}_{\nu_L} U = \mathrm{diag}(m_1, m_2, m_3)\,. \tag{2.5}$$

Here, U is the Pontecorvo-Maki-Nakagawa-Sakata (PMNS) mixing matrix U [51–54] and can be parameterised as [55]

$$U = \begin{pmatrix} c_{12}c_{13} & s_{12}c_{13} & s_{13}e^{-i\delta} \\ -s_{12}c_{23} - c_{12}s_{23}s_{13}e^{i\delta} & c_{12}c_{23} - s_{12}s_{23}s_{13}e^{i\delta} & s_{23}c_{13} \\ s_{12}s_{23} - c_{12}c_{23}s_{13}e^{i\delta} & -c_{12}s_{23} - s_{12}c_{23}s_{13}e^{i\delta} & c_{23}c_{13} \end{pmatrix} \times \begin{pmatrix} 1 & 0 & 0 \\ 0 & e^{i\frac{\alpha_2}{2}} & 0 \\ 0 & 0 & e^{i\frac{\alpha_3}{2}} \end{pmatrix}, \tag{2.6}$$

where $c_{ij} \equiv \cos\theta_{ij}$ and $s_{ij} \equiv \sin\theta_{ij}$ and δ, α_2, $\alpha_3 \in [0, 2\pi]$. The Normal Ordering (NO) of neutrino masses, where $m_1 < m_2 < m_3$, is the only mass hierarchy that is consistent with neutrino oscillation data in this model, as demonstrated in ref. [21].

Using eqs. (2.4) and (2.5), it is possible to express the Majorana mass matrix $\mathcal{M}_R$ as

$$\mathcal{M}_R = -\mathcal{M}_D^T\, U\, \mathrm{diag}(m_1^{-1}, m_2^{-1}, m_3^{-1})\, U^T \mathcal{M}_D\,. \tag{2.7}$$

The (μ,μ) and (τ,τ) components of the right-hand side of the above equation vanish. This is a direct consequence of the two-zero-minor structure [49, 50] of $\mathcal{M}_{\nu_L}$ in this model.[2] The vanishing conditions on complex quantities result in four real parameter equations. These equations allow us to predict the values of the lightest neutrino mass m_1, as well as the Dirac and Majorana CP phases δ, α_2, and α_3, as functions of the other neutrino oscillation parameters. These parameters include the neutrino mixing angles θ_{12}, θ_{23}, θ_{13}, and the squared mass differences $\Delta m^2_{21} \equiv m_2^2 - m_1^2$, and $\Delta m^2_{31} \equiv m_3^2 - m_1^2$. For each set of input parameters, there exist two possible sets of predictions, as shown in ref. [21]. Specifically, if the set (m_1, δ, α_2, α_3) satisfies the two-vanishing conditions, then the set (m_1, $2\pi - \delta$, $2\pi - \alpha_2$, $2\pi - \alpha_3$) also satisfies them.

For our numerical study, we fix the neutrino mixing angles and the squared mass differences following the `NuFit` analyses [56], which are comprehensive global fits that include data from all the relevant neutrino oscillation experiments. The most recent `NuFit` analyses are conducted both with and without incorporating data from the Super-Kamiokande (SK) experiment. These two approaches yield somewhat different values for the neutrino mixing angles and squared mass differences. We summarise the results obtained in the `NuFit 5.2` analysis [56, 57] for the best-fit values, 1σ deviations and 3σ ranges of the neutrino mixing angles and mass squared differences in table 2.

We observe that, while the inclusion of the SK data substantially affects the best-fit $\pm1\sigma$ values of θ_{23}, it does not change dramatically its 3σ allowed range (the maximal value without SK data is larger by 0.9°) and the results for θ_{12}, θ_{13}, Δm^2_{21}, and Δm^2_{31}. Specifically, the best fit $\pm1\sigma$ values for θ_{23} lie below (above) $\pi/4$ with (without) the inclusion of SK data. Since the minimal gauged $\mathrm{U}(1)_{L_\mu - L_\tau}$ model predictions are highly dependent on the value of θ_{23}, as the sum of neutrino masses diverges for $\theta_{23} = \pi/4$ [21], we examine the cases

[2] Note that this structure is stable against the renormalisation-group effects [21].

JHEP09(2023)079

Neutrino Masses and Mixing Parameters					
Parameters	θ_{12}	θ_{13}	θ_{23}	Δm^2_{21}	Δm^2_{31}
(units)	$(^\circ)$	$(^\circ)$	$(^\circ)$	$(10^{-5}\ \mathrm{eV}^2)$	$(10^{-3}\ \mathrm{eV}^2)$
With SK	$33.41^{+0.75}_{-0.72}$	$8.58^{+0.11}_{-0.11}$	$42.2^{+1.1}_{-0.9}$	$7.41^{+0.21}_{-0.20}$	$2.507^{+0.026}_{-0.027}$
3σ range	$[31.31, 35.74]$	$[8.23, 8.91]$	$[39.7, 51.0]$	$[6.82, 8.03]$	$[2.427, 2.590]$
Without SK	$33.41^{+0.75}_{-0.72}$	$8.54^{+0.11}_{-0.12}$	$49.1^{+1.0}_{-1.3}$	$7.41^{+0.21}_{-0.20}$	$2.511^{+0.028}_{-0.027}$
3σ range	$[31.31, 35.74]$	$[8.19, 8.89]$	$[39.6, 51.9]$	$[6.82, 8.03]$	$[2.427, 2.590]$

Table 2. Best-fit values, 1σ deviations and 3σ allowed ranges of the neutrino mixing angles θ_{12}, θ_{13}, θ_{23}, and of the squared mass differences Δm^2_{21} and Δm^2_{31} in the case of NO light neutrino mass spectrum, from the latest `NuFit 5.2` analysis [56, 57]. The two lines of values correspond to the fit with (top) and without (bottom) the inclusion of SK data.

with and without the inclusion of SK data separately.[3] In both cases, we set θ_{12}, θ_{13}, Δm^2_{21}, and Δm^2_{31} to their best-fit values, while we treat θ_{23} differently given the implications it has on the sum of neutrino masses predicted by the considered model.

The sum of the neutrino masses is constrained by various cosmological and astrophysical measurements, yielding an upper bound of $\sum_i m_i < (0.12\text{–}0.69)\,\mathrm{eV}$ (95% C.L.), which depends on the adopted model and level of statistical complexity [58, 59] (see also refs. [1, 60–64]). By adopting the best-fit values for θ_{23} in the two cases with and without SK data, we obtain $\sum_i m_i \simeq 0.241\,\mathrm{eV}$ and $0.173\,\mathrm{eV}$, respectively. However, in order to evade the aforementioned limitations, some level of complexity and assumptions is required. We instead set θ_{23} to its $-\,(+)\,3\sigma$ minimal (maximal) limit for the case with (without) SK data; specifically, $\theta_{23} = 39.7^\circ\,(51.9^\circ)$, with the other input parameters at their best-fit values. This yields $\sum_i m_i = 0.142\,(0.117)$ eV, which minimises the sum of neutrino masses and reduces the tension with the cosmological bounds. To summarise, in our numerical analysis, we consider the following two sets of input parameters:

Set I	**Set II**
$\theta_{12} = 33.41^\circ$	$\theta_{12} = 33.41^\circ$
$\theta_{13} = 8.58^\circ$	$\theta_{13} = 8.54^\circ$
$\theta_{23} = 39.7^\circ$	$\theta_{23} = 51.9^\circ$
$\Delta m^2_{21} = 7.41 \times 10^{-5}\,\mathrm{eV}^2$	$\Delta m^2_{21} = 7.41 \times 10^{-5}$
$\Delta m^2_{31} = 2.507 \times 10^{-3}\,\mathrm{eV}^2$	$\Delta m^2_{31} = 2.511 \times 10^{-3}\,\mathrm{eV}^2$.

The minimal gauged $\mathrm{U}(1)_{L_\mu - L_\tau}$ model, when combined with the neutrino mixing angles and squared mass differences in Set I (II), predicts a value of $m_1 = 0.039\,(0.029)\,\mathrm{eV}$.[4] In

[3] See figure 1(b) in ref. [24], in which the sum of neutrino masses as a function of θ_{23} is shown. For such figure, the authors of ref. [24] adopted an older version of the neutrino oscillation data (`NuFit 4.1`), but the behaviour of the same function in our case remains basically the same.

[4] The model also makes predictions about the effective Majorana mass $\langle m_{\beta\beta}\rangle$ which determines the rate of the neutrinoless double-beta decay. The parameter set I (II) predicts $\langle m_{\beta\beta}\rangle \simeq 0.025\,\mathrm{eV}$ $(0.016\,\mathrm{eV})$, which is below the current constraint given by the KamLAND-Zen experiment, $\langle m_{\beta\beta}\rangle < 0.036\text{–}0.156\,\mathrm{eV}$ [65], and may be probed by future experiments with sensitivities of $\langle m_{\beta\beta}\rangle \simeq \mathcal{O}(0.01)\,\mathrm{eV}$ [66, 67].

JHEP09(2023)079

addition, the PMNS phases are determined to be $\delta \simeq 301^\circ\,(228^\circ)$, $\alpha_2 = 116^\circ\,(225^\circ)$ and $\alpha_3 = 269^\circ\,(70^\circ)$, or equivalently, $\delta = 59^\circ\,(132^\circ)$, $\alpha_2 = 244^\circ\,(135^\circ)$ and $\alpha_3 = 91^\circ\,(290^\circ)$. The Dirac phase δ has also been estimated by the `NuFit` analysis, which reports a 3σ range of $[144^\circ, 350^\circ]$ when including SK data, and $[0, 44^\circ] \cup [108^\circ, 360^\circ]$ when not including it. Consequently, the set of parameters of Set I with $\delta = 59^\circ$ is disfavoured for more than 3σ.

By specifying the three additional input parameters in the Dirac mass matrix, $\mathcal{M}_D = (v/\sqrt{2})\mathrm{diag}(\lambda_e, \lambda_\mu, \lambda_\tau)$, it is possible to obtain the right-handed neutrino mass matrix $\mathcal{M}_R$. These Yukawa couplings are parameterised, according to ref. [21], as

$$(\lambda_e, \lambda_\mu, \lambda_\tau) = \lambda(\cos\theta, \sin\theta\cos\phi, \sin\theta\sin\phi), \tag{2.8}$$

where we consider the range of $0 \leq \theta\,\mathrm{and}\,\phi \leq \pi/2$. We also limit the value of λ to $\lambda \lesssim 1$ to ensure that the Yukawa couplings remain perturbative. The masses of the right-handed neutrinos are obtained by performing the Takagi diagonalisation on the complex symmetric matrix $\mathcal{M}_R$

$$\mathcal{M}_R = \Omega^* \mathrm{diag}(M_1, M_2, M_3)\Omega^\dagger, \tag{2.9}$$

where Ω is a unitary matrix and $M_{1,2,3} \geq 0$. Once the mass matrix of the right-handed neutrinos $\mathcal{M}_R$ is diagonalised, the terms in eq. (2.1) lead to

$$\Delta\mathcal{L} = -\hat{\lambda}_{j\alpha}\hat{N}^c_j(\ell_\alpha \cdot H) - \frac{1}{2}M_j\hat{N}^c_j\hat{N}^c_j + \mathrm{h.c.}\,, \tag{2.10}$$

where the sum over equal indices is implicit and

$$\hat{N}^c_j = \sum_\alpha \Omega^*_{\alpha j} N^c_\alpha\,, \tag{2.11}$$

$$\hat{\lambda}_{j\alpha} = \Omega_{\alpha j}\lambda_\alpha \text{ (not summed)}. \tag{2.12}$$

The Weyl spinor $\hat{N}_j$, $j = 1, 2, 3$, with $(\hat{N}^c_j)_a = \varepsilon_{ab}(\hat{N}^*_j)_b$, describes a right-handed neutrino N_j with mass M_j.

Upon examining eq. (2.7) and using the Yukawa coupling parameterisation provided in eq. (2.8), it becomes transparent that the masses of the right-handed neutrinos are proportional to λ^2. This dependence can be expressed more precisely as follows,

$$M_{1,2,3} = \frac{v^2\lambda^2}{2m_1}\,\beta_{1,2,3}(\theta,\phi) \simeq 6\times 10^{14}\,\mathrm{GeV}\left(\frac{0.05\,\mathrm{eV}}{m_1}\right)\lambda^2\beta_{1,2,3}(\theta,\phi), \tag{2.13}$$

where $\beta_{1,2,3}(\theta,\phi)$, satisfying $\beta_{1,2,3}(\theta,\phi) \lesssim \mathcal{O}(1)$, are some real numbers that only depend on the ratios $m_1/m_2 < 1$, $m_1/m_3 < 1$, the PMNS parameters and on trigonometric functions of θ, ϕ.[5]

Figure 1 shows the contours for three parameters: $\beta_1 = 2m_1v^{-2}\lambda^{-2}M_1$ (top), $\beta_2/\beta_1 - 1 = \Delta M_{21}/M_1$ (bottom-left), and $\beta_3/\beta_2 - 1 = \Delta M_{32}/M_2$ (bottom-right); here, $\Delta M_{21(32)} \equiv M_{2(3)} - M_{1(2)}$. These contours are obtained using the neutrino mixing angles and squared mass differences as in Set I, with ϕ and θ varied in the $\pi/2$ range with $0 \leq \theta,\, \phi \leq \pi/2$. We observe that the parameter β_1 exhibits a maximum value of $\beta_1^{\max} \sim 0.24$ at the location

[5]More precisely, $\beta_{1,2,3}(\theta,\phi)$ are defined by $\mathrm{diag}(\beta_1,\beta_2,\beta_3) = -\Omega^T D_{\theta,\phi}UD_mU^TD_{\theta,\phi}\Omega$, where $D_{\theta,\phi} \equiv \mathrm{diag}(\cos\theta, \sin\theta\cos\phi, \sin\theta\sin\phi)$ and $D_m \equiv \mathrm{diag}(1, m_1/m_2, m_1/m_3)$.

JHEP09(2023)079

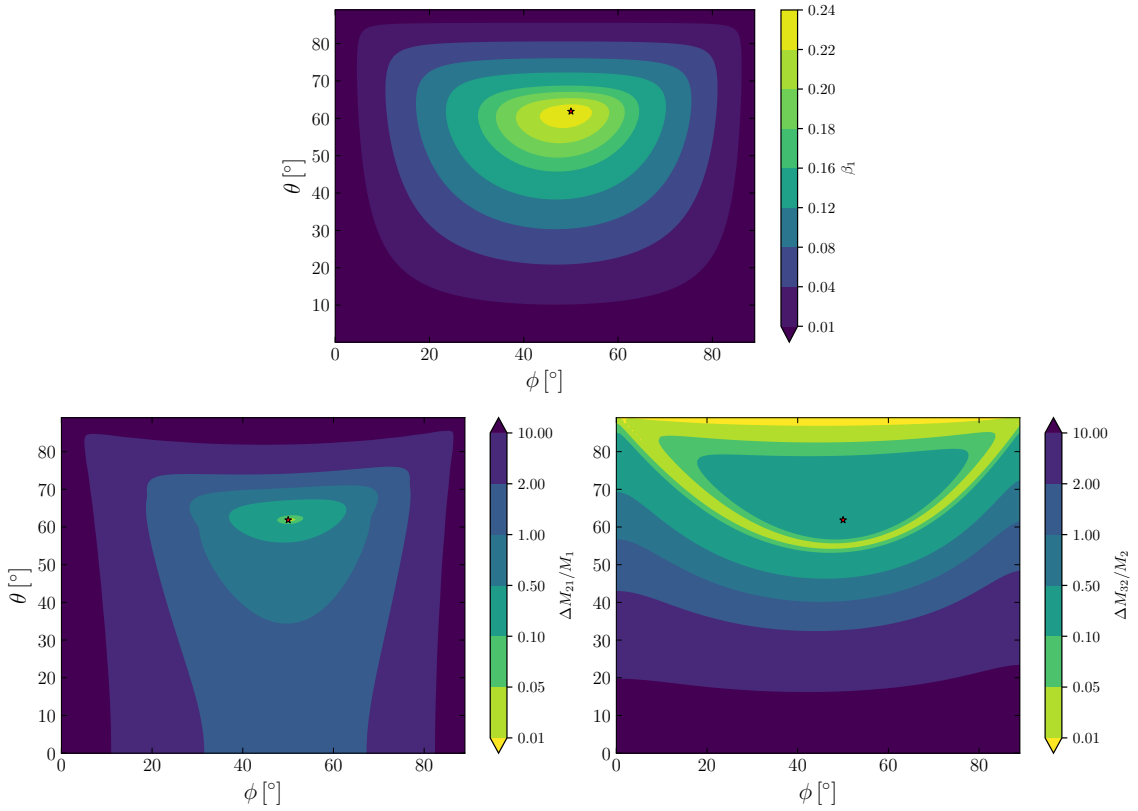

Figure 1. The contour plots for the quantities β_1 (top panel), $\Delta M_{21}/M_1$ (bottom-left panel) and $\Delta M_{32}/M_2$ (bottom-right panel) in the $\phi - \theta$ plane. The red stars in the plots mark the point of coordinates $\phi \sim 50°$ and $\theta \sim 62°$ for which β_1 is maximised ($\Delta M_{21}/M_1$ is minimised). The plot is obtained for the neutrino mixing angles, and squared mass differences as in Set I. Choosing the input parameters as in Set II would lead to a qualitatively similar figure.

with coordinates $\phi = \tilde{\phi} \sim 50°$ and $\theta = \tilde{\theta} \sim 62°$, which is marked with a red star. At the same coordinates, we find numerically that $\Delta M_{21}/M_1$ is minimised, while $\Delta M_{32}/M_2$ is locally maximised. Moreover, we find that the overall trend of the parameter space remains consistent if we choose to work with the values for θ_{12}, θ_{13}, Δm^2_{21} and Δm^2_{31} as in Set II. However, the maximum value of β_1 is found for different values of ϕ and θ. Specifically, the maximum value of β_1 is found at $\phi = \tilde{\phi} \sim 38°$ and $\theta = \tilde{\theta} \sim 65°$, taking a value of ~ 0.21. Upon examining the bottom panels of figure 1, it is evident that our model predicts a nearly degenerate spectrum for the right-handed neutrinos, with $M_2 \lesssim 3M_1$ and $M_3 \lesssim 3M_2$, over a large part of the parameter space. However, we do not observe all three right-handed neutrinos to be simultaneously nearly-degenerate in mass in any region of the parameter space. There exists a tiny region where N_1 and N_2 are nearly-degenerate with $M_2 \lesssim 1.05M_1$. For N_2 and N_3, there exists a larger region nearly degenerate, with $M_3 \lesssim 1.05M_2$. These regions are shown in yellow-ish colour in the bottom panels of figure 1.[6]

[6]We suspect that a specific point for which $M_1 = M_2$ exists around $(\tilde{\phi}, \tilde{\theta})$ (although finding such precise point would require infinite numerical resolution). It should be possible to consider $M_1 \simeq M_2$ with arbitrary precision around that point, but this would require a certain amount of fine-tuning in the choice of the parameters θ and ϕ, much more severe than, e.g., the uncertainties in the neutrino parameters we have considered.

JHEP09(2023)079

3 Thermal leptogenesis

In this section, we present the equations necessary to investigate the thermal leptogenesis mechanism in the minimal gauged $\mathrm{U}(1)_{L_\mu - L_\tau}$ model. To simplify our analysis, we make the following assumptions: i) the $\mathrm{U}(1)_{L_\mu - L_\tau}$ gauge symmetry is never restored after the reheating; ii) the masses of the $\mathrm{U}(1)_{L_\mu - L_\tau}$ gauge boson and the singlet scalar field associated with σ are larger than the reheating temperature T_R so that these fields are always absent from the thermal bath; iii) the masses of all three right-handed neutrinos are smaller than the reheating temperature. The first two can be realised by taking the $\mathrm{U}(1)_{L_\mu - L_\tau}$ gauge coupling and the self coupling of the σ field sufficiently large and $\langle\sigma\rangle \gg T_R$. The third assumption indicates $|M_{ee,\mu\tau}|, |\lambda_{e\mu,e\tau}\langle\sigma\rangle| < T_R$.

To take the impact of charged lepton and heavy neutrino flavours into account, we employ the formalism of DMEs instead of the simpler BEs.[7] Specifically, in the case of the three decaying right-handed neutrinos, we can express the DMEs in the following compact form [40–42, 44, 45, 68]:

$$\frac{dN_{N_j}}{dz} = -D_j(N_{N_j} - N_{N_j}^{\mathrm{eq}})\,, \tag{3.1}$$

$$\begin{aligned}\frac{dN_{\alpha\beta}}{dz} = &\sum_{j=1}^{3}\left[\epsilon_{\alpha\beta}^{(j)} D_j(N_{N_j} - N_{N_j}^{\mathrm{eq}}) - \frac{1}{2}W_j\left\{P^{0(j)}, N\right\}_{\alpha\beta}\right] \\ &- \frac{\Gamma_\tau}{Hz}\left[I_\tau, [I_\tau, N]\right]_{\alpha\beta} - \frac{\Gamma_\mu}{Hz}\left[I_\mu, [I_\mu, N]\right]_{\alpha\beta}\,,\end{aligned} \tag{3.2}$$

where the indices $j = 1, 2, 3$ refer to the three decaying right-handed neutrinos, while $\alpha, \beta = e, \mu, \tau$ to the charged lepton flavours. The variable z is defined as $z \equiv M_1/T$. The quantity N_{N_j} represents the number of heavy neutrinos N_j in a comoving volume, which we normalise using the same method as in refs. [44, 45, 68], such that it contains a single photon when $z \ll 1$, i.e., $N_{N_j}^{\mathrm{eq}}(0) = 3/4$. We approximate the equilibrium number density of heavy neutrinos as $N_{N_j}^{\mathrm{eq}}(z) = (3/8)x_j z^2 K_2(\sqrt{x_j}z)$, where $x_j \equiv (M_j/M_1)^2$ and $K_n(z)$, $n = 1, 2, \ldots$, is the modified n^{th} Bessel function of the second kind [33, 70]. The diagonal entries $N_{\alpha\alpha}$ of the density matrix N correspond to the comoving number densities for the $(1/3)B - L_\alpha$ asymmetry, such that $N_{B-L} = \sum_{\alpha=e,\,\mu,\,\tau} N_{\alpha\alpha}$. The off-diagonal elements $N_{\alpha\beta}$, where $\alpha \neq \beta$, represent the degree of coherence between the flavour states.

The projection matrices in the anti-commutator term in the first line of eq. (3.2) is defined as,

$$P_{\alpha\beta}^{0(j)} \equiv \frac{\hat{\lambda}_{j\alpha}^{*}\hat{\lambda}_{j\beta}}{(\hat{\lambda}\hat{\lambda}^{\dagger})_{jj}}\,, \tag{3.3}$$

[7] Charged lepton and heavy neutrino flavour effects can be particularly relevant when the right-handed neutrino mass is not strongly hierarchical [42], as in our model (see figure 1). In addition, as we will show later, to explain the observed BAU, the mass of the lightest right-handed neutrino can be as low as $M_1 \sim 10^{11-12}$ GeV, with leptogenesis occurring at the transition between the single- and two-flavour regimes, where BEs fail [68, 69]. Therefore, it is necessary to solve the DMEs with three decaying right-handed neutrinos and fully take flavour effects into account.

JHEP09(2023)079

generalising the notion of the projection probability. Furthermore, the double commutator structure in the second line of eq. (3.2) involves 3×3 matrices I_τ and I_μ defined such that $(I_\tau)_{\alpha\beta} = \delta_{\alpha\tau}\delta_{\beta\tau}$ and $(I_\mu)_{\alpha\beta} = \delta_{\alpha\mu}\delta_{\beta\mu}$. Additionally, we use the following analytical expressions for D_j and W_j [33, 44],

$$D_j(z) = \kappa_j x_j z \frac{K_1(\sqrt{x_j}z)}{K_2(\sqrt{x_j}z)}\,, \tag{3.4}$$

$$W_j(z) = \frac{1}{4}\kappa_j x_j^2 z^3 K_1(\sqrt{x_j}z)\,, \tag{3.5}$$

where the decay parameter κ_j quantifies the strength of the wash-out processes in erasing the asymmetry and is defined as the ratio between the total decay rate of N_j at zero temperature, $\Gamma_j = (\hat{\lambda}\hat{\lambda}^\dagger)_{jj} M_j/8\pi$, and the Hubble expansion rate H at $T = M_j$. Note that the decay rate Γ_j and the Hubble expansion rate $H(T = M_j) \propto M_j^2$ scale as λ^4. As a result, the decay parameter κ_j depends only on the angles θ and ϕ. Numerical calculations show that, for any $0 \leq \theta,\, \phi \leq \pi/2$ and $j = 1,\, 2,\, 3$, $\kappa_j \gg 1$ and leptogenesis occurs in the strong wash-out regime.[8]

To solve the DMEs, we need to specify the right-handed neutrino abundances and lepton asymmetries at the starting point of leptogenesis $z_{\rm in}$. The strong wash-out condition $\kappa_i \gg 1$ itself does not guarantee the independence of the initial conditions. With strong wash-outs occurring for each lepton flavour, the final BAU is not affected by different choices of the initial abundances [71]. Nonetheless, it can still be, for instance, that one or two lepton flavours are weakly coupled, and the independence of the initial condition is not guaranteed [72]. While it is natural to assume that the Universe was symmetric in the lepton and baryon numbers at the beginning of leptogenesis, with all the entries of the flavour density matrix equal to zero, there is more freedom in the choice of the initial right-handed neutrino abundances. In the main analysis, we focus on the case for which the starting abundances of the right-handed neutrinos are zero, as this situation is generically more natural in cosmological inflation models. We dedicate appendix A to discuss how our results change with thermal initial abundances.

It has also been estimated that, in the strong wash-out regime and in the case of a hierarchical right-handed neutrino mass spectrum, the $\Delta L = 1$ scattering processes and related wash-outs would only contribute to the final BAU at most by $\mathcal{O}(10\%)$ [71, 73]. We find that this is still true in most of the parameter space of our model, except for certain fine-tuned choices of the parameters. Therefore, we do not consider the effects of scatterings in the main analysis.[9]

The CP-asymmetry $\epsilon^{(j)}_{\alpha\beta}$ appearing in the DMEs can be separated into contributions from vertex and self-energy diagrams, namely $\epsilon^{(j)}_{\alpha\beta} \equiv \epsilon^{{\rm V}\,(j)}_{\alpha\beta} + \epsilon^{{\rm S}\,(j)}_{\alpha\beta}$. The two contributions

[8] More specifically, we find numerically that $\kappa_i \gtrsim 40$ and can reach maximal values of $\kappa_1 \simeq 1.66 \times 10^2$ and $\kappa_{2,3} \simeq 1.41 \times 10^4$.

[9] We are neglecting from our analysis the contributions to the BAU from the early period when the right-handed neutrinos are relativistic and the effects of spectator processes that could potentially affect our final results (see, e.g., [74] and references therein). We leave the implementation of these effects to future related studies.

JHEP09(2023)079

are given by [38, 40, 42, 75–79],

$$\epsilon^{\mathrm{V}\,(j)}_{\alpha\beta} = \frac{1}{16\pi\left(\hat{\lambda}\hat{\lambda}^{\dagger}\right)_{jj}} \sum_{k\neq j} \left\{ i\left[\hat{\lambda}^{*}_{j\alpha}\hat{\lambda}_{k\beta}(\hat{\lambda}\hat{\lambda}^{\dagger})_{kj} - \hat{\lambda}_{j\beta}\hat{\lambda}^{*}_{k\alpha}(\hat{\lambda}\hat{\lambda}^{\dagger})_{jk}\right] \xi\left(x_k/x_j\right)\right\} , \tag{3.6}$$

$$\begin{aligned}\epsilon^{\mathrm{S}\,(j)}_{\alpha\beta} = \frac{1}{16\pi\left(\hat{\lambda}\hat{\lambda}^{\dagger}\right)_{jj}} \sum_{k\neq j} \Bigg\{ & i\left[\hat{\lambda}^{*}_{j\alpha}\hat{\lambda}_{k\beta}(\hat{\lambda}\hat{\lambda}^{\dagger})_{kj} - \hat{\lambda}_{j\beta}\hat{\lambda}^{*}_{k\alpha}(\hat{\lambda}\hat{\lambda}^{\dagger})_{jk}\right] \frac{\sqrt{x_k/x_j}}{x_k/x_j - 1} \\ & + i\left[\hat{\lambda}^{*}_{j\alpha}\hat{\lambda}_{k\beta}(\hat{\lambda}\hat{\lambda}^{\dagger})_{jk} - \hat{\lambda}_{j\beta}\hat{\lambda}^{*}_{k\alpha}(\hat{\lambda}\hat{\lambda}^{\dagger})_{kj}\right] \frac{1}{x_k/x_j - 1} \Bigg\} ,\end{aligned} \tag{3.7}$$

where $\xi(x) \equiv \sqrt{x}\left[(1+x)\log\left(1+1/x\right) - 1\right]$. In the case of a degeneracy in the right-handed neutrino mass spectrum, the self-energy contribution to the CP-asymmetry is resonantly enhanced and can dominate over the vertex contribution. However, the self-energy contribution in eq. (3.7) becomes ill-defined when two neutrinos, say N_j and N_k, are quasi-degenerate in mass, as $1/(x_k/x_j - 1) \to \infty$ when $x_k/x_j \to 1$. To address this non-physical behaviour, the full-resummed Yukawa couplings must be considered in the calculations, and the self-energy contribution to the CP-asymmetry can be regularised by performing the following substitution [80–83],

$$\frac{1}{x_k/x_j - 1} \to \frac{(M_k^2 - M_j^2)M_j^2}{(M_k^2 - M_j^2)^2 + M_j^4\Gamma_k^2/M_k^2} \,. \tag{3.8}$$

The regularised CP-asymmetry, obtained by using the prescription in eq. (3.8), does not suffer from divergences and vanishes for equal right-handed neutrino masses. However, the self-energy contribution to the CP-asymmetry, even after regularisation, still exhibits a resonance. In particular, the self-energy contribution is maximised when $|\Delta M_{jk}| \simeq 0.5\,\Gamma_j$, with $\Delta M_{jk} \equiv M_j - M_k$. This resonant behaviour has been extensively studied in the context of resonant leptogenesis, especially in the efforts to avoid the Davidson-Ibarra bound [29] and extend the scenario of thermal leptogenesis down to the electroweak scale [69, 80–92]. A comprehensive review can be found in ref. [93]. The ratios $|\Delta M_{jk}|/\Gamma_j$, $j \neq k$, quantify the importance of resonance effects. Far away from the resonance, when $|M_j - M_k| \gg \Gamma_j$, the effects of the enhancement are sub-leading, and the regularised CP-asymmetry obtained with the prescription in eq. (3.8) resembles the form given in eq. (3.7). We perform a scan of $|\Delta M_{12}|/\Gamma_1$ and $|\Delta M_{23}|/\Gamma_2$ over the $\phi - \theta$ plane for various choices of λ. We found that resonance effects are significant only in certain small regions of the parameter space. Furthermore, these regions become even smaller with decreasing values of λ and are effectively negligible when $\lambda \lesssim 0.5$. The details of this analysis can be found in appendix B. Nevertheless, we have included the effects of resonance as in eq. (3.8) in our calculations.[10]

[10]Different approaches to regularise the self-energy contribution to the CP-asymmetry have been proposed [93–95]. However, in our case, the mass splittings between the right-handed neutrinos are much larger than their decay widths and we expect that a different estimation of the resonant effects would not significantly affect our results. It is worth noting that in ref. [82] (and in the recent study in ref. [96]), a more sophisticated regularisation taking into account the mass degeneracy between all the three right-handed neutrinos was found. However, our analysis presented in appendix B shows no region of the parameter space of our model for which $|M_1 - M_2|/\Gamma_1 \lesssim 10$ and $|M_2 - M_3|/\Gamma_2 \lesssim 10$ simultaneously. Hence, for our purposes, it is sufficient to consider the mass degeneracy between two right-handed neutrinos at a time and use the simplified regularisation in eq. (3.8).

JHEP09(2023)079

Finally, we numerically solve the DMEs in eqs. (3.1) and (3.2) with the Python package `ULYSSES` [46, 47]. The code computes $N_{B-L} = N_{ee} + N_{\mu\mu} + N_{\tau\tau}$ and relates it to the present baryon-to-photon ratio via

$$\eta_B = \frac{c_s}{f} N_{B-L} \approx 0.013 N_{B-L} \,, \tag{3.9}$$

where c_s is the SM sphaleron conversion coefficient and the f factor comes from the dilution of the baryon asymmetry due to the change in the photon density between leptogenesis and recombination [33].

4 Results of the parameter scan of viable leptogenesis

In this section, we discuss the results of our parameter scan aimed at identifying the viable space for thermal leptogenesis by solving the set of DMEs introduced in section 3 in the case of vanishing right-handed neutrino initial abundances. Figure 2 shows the results of the scan in the $\phi - \theta$ plane for three benchmark values of λ, namely $\lambda = 0.5$ (top panels), $\lambda = 0.3$ (central panels) and $\lambda = 0.1$ (bottom panels). The plots in the left and right panels are obtained with the neutrino mixing angles and squared mass differences as in Set I with $(\delta,\, \alpha_2,\, \alpha_3) = (301^\circ,\, 116^\circ,\, 269^\circ)$ and Set II with $(\delta,\, \alpha_2,\, \alpha_3) = (228^\circ,\, 225^\circ,\, 70^\circ)$, respectively. The regions of viable leptogenesis are those surrounded by the solid red contours, where the predicted BAU matches the observed value $\eta_B = 6.1 \times 10^{-10}$. The points corresponding to the dotted red contours result in a predicted BAU of -6.1×10^{-10}, indicating the correct magnitude but wrong sign. To darker (lighter) regions correspond larger (smaller) values of the predicted BAU, in modulus.

In figure 2, it is clear that there are numerous regions in the parameter space where leptogenesis within the minimal gauged $\mathrm{U}(1)_{L_\mu - L_\tau}$ model predicts a BAU equal to or greater than the observed value, in modulus. However, the sign of the BAU alternates between positive and negative values in different regions, and only those regions where the BAU is positive correspond to successful leptogenesis. It is worth noting that the sign of the BAU can always be changed without changing its magnitude by switching to the equivalent solution with $(m_1,\, 2\pi - \delta,\, 2\pi - \alpha_2,\, 2\pi - \alpha_3)$ [21]. This can be shown as follows. First, note that switching from a set of solutions $(m_1,\, \delta,\, \alpha_2,\, \alpha_3)$ to the other one $(m_1,\, 2\pi - \delta,\, 2\pi - \alpha_2,\, 2\pi - \alpha_3)$ yields $U \to U^*$, and thus $\mathcal{M}_{\nu_L} \to \mathcal{M}^*_{\nu_L}$, $\mathcal{M}_R \to \mathcal{M}^*_R$, $\Omega \to \Omega^*$, and $\hat{\lambda} \to \hat{\lambda}^*$. Then, $\epsilon^{(j)}_{\alpha\beta}$ and $P^{0(j)}_{\alpha\beta}$ in eq. (3.2) transform as $\epsilon^{(j)}_{\alpha\beta} \to -\epsilon^{(j)}_{\beta\alpha}$ and $P^{0(j)}_{\alpha\beta} \to P^{0(j)}_{\beta\alpha}$, respectively. This indicates that if N_{N_j} and $N_{\alpha\beta}$ are solutions of eqs. (3.1) and (3.2) for a given set of $(m_1,\, \delta,\, \alpha_2,\, \alpha_3)$, then the solutions for $(m_1,\, 2\pi - \delta,\, 2\pi - \alpha_2,\, 2\pi - \alpha_3)$ are given by N_{N_j} and $-N_{\beta\alpha}$. By noting that $\eta_B \propto (N_{ee} + N_{\mu\mu} + N_{\tau\tau})$, we conclude that if the baryon-to-photon ratio for $(m_1,\, \delta,\, \alpha_2,\, \alpha_3)$ is given by η_B, that for $(m_1,\, 2\pi - \delta,\, 2\pi - \alpha_2,\, 2\pi - \alpha_3)$ is given by $-\eta_B$. It is also important to note that there is an overall sign difference between the parameter scans obtained for the two sets of input parameters, Set I and II. This is because θ_{23} varies from values below 45° in Set I to values above 45° in Set II, resulting in a shift in the PMNS phases and an opposite sign of the BAU.[11] Consequently, only precise

[11] The behaviour is not exactly symmetric in θ_{23}, see figure 1(b) of ref. [24].

JHEP09(2023)079

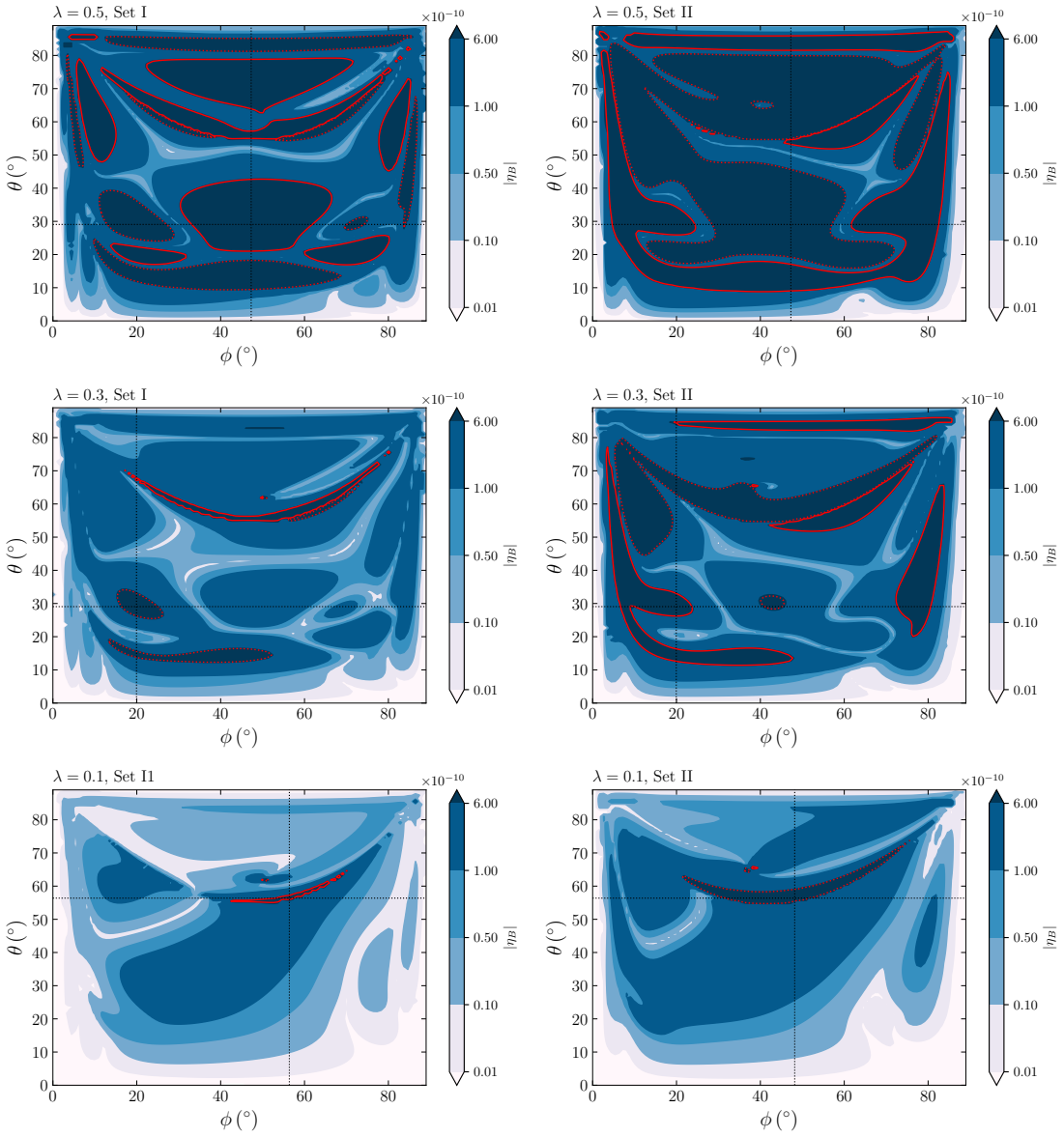

Figure 2. The contour plots in the $\phi - \theta$ plane of the BAU (in modulus) predicted by the DMEs with three decaying right-handed neutrinos in the case of vanishing initial abundances. The plots are obtained for $\lambda = 0.5$ (top panels), 0.3 (central panels) and 0.1 (bottom panels), with the input parameters θ_{12}, θ_{13}, θ_{23}, Δm^2_{21} and Δm^2_{31} as in Set I with $(\delta, \alpha_2, \alpha_3) = (301°, 116°, 269°)$ (left panels) and Set II with $(\delta, \alpha_2, \alpha_3) = (228°, 225°, 70°)$ (right panels). As indicated in the bar legends, darker (lighter) regions correspond to larger (smaller) values of the BAU, with the red solid contours representing the points for which the predicted BAU equals the observed value $\eta_B \simeq 6.1 \times 10^{-10}$. For the red dotted contours, the BAU equals the observed value in modulus, but the sign is negative. The dotted vertical and horizontal lines mark the benchmark points BMPa (top panels), BMPb (central panels), BMPcI and BMPcII (bottom panels).

JHEP09(2023)079

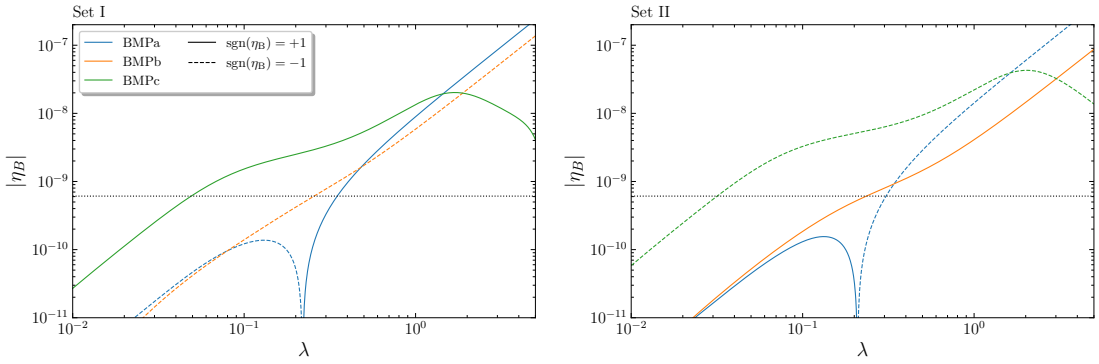

Figure 3. The BAU as a function of λ predicted by the DMEs with three decaying right-handed neutrinos. The input parameters in the left and right panels are as in Set I with $(\delta,\, \alpha_2,\, \alpha_3) = (301°,\, 116°,\, 269°)$ and Set II with $(\delta,\, \alpha_2,\, \alpha_3) = (228°,\, 225°,\, 70°)$, respectively. The different curves are obtained for BMPa (blue), BMPb (orange), BMPcI and BMPcII (green), with the solid (dashed) style indicating the positive (negative) sign of the predicted baryon-to-photon ratio. Note the overall sign flip between the curves obtained in the two different sets of input parameters.

combinations of the phase δ and mixing angle θ_{23} can lead to the correct sign of the BAU in a particular point of the $\phi - \theta$ plane. Determining whether $\theta_{23} <$ or $> \pi/4$ and/or $\delta <$ or $> \pi$ in future experiments would rule out certain regions of the parameter space of viable leptogenesis in our model only based on the sign of the predicted baryon-to-photon ratio.

In addition, the size of the allowed regions for successful leptogenesis in the $\phi - \theta$ plane is dependent on the mass scale of leptogenesis, which goes as λ^2. As λ decreases (increases), the allowed ranges of ϕ and θ for successful leptogenesis become smaller (larger). To determine the minimal values of λ at which the viable regions shrink to points, we search for the local maxima of the predicted BAU. We identify four benchmark points (BMPs) in the $\phi - \theta$ plane, around which the symmetry is locally maximised. The BMPs are located at the coordinates BMP a) $\theta = 29.06°$ and $\phi = 47.28°$; BMP b) $\theta = 29.06°$ and $\phi = 19.94°$; BMP cI) $\theta = 56.39°$ and $\phi = 56.39°$ for Set I, and BMP cII) $\theta = 56.39°$ and $\phi = 48.19°$ for Set II. These four BMPs are indicated in figure 2 by horizontal and vertical dotted grid lines.

Finally, figure 3 illustrates the dependence of the BAU on the scale λ for the four different BMPs. The left and right panels correspond to input parameters as in Set I with $(\delta,\, \alpha_2,\, \alpha_3) = (301°,\, 116°,\, 269°)$ and Set II with $(\delta,\, \alpha_2,\, \alpha_3) = (228°,\, 225°,\, 70°)$, respectively. Our numerical analysis yields the following minimal values of λ for which leptogenesis is viable: for Set I, $\lambda \simeq 0.35$ ($M_1 \simeq 10^{12.8}\,\text{GeV}$) for BMPa and $(\delta,\, \alpha_2,\, \alpha_3) = (301°,\, 116°,\, 269°)$; $\lambda \simeq 0.25$ ($M_1 \simeq 10^{12.2}\,\text{GeV}$) for BMPb and $(\delta, \alpha_2, \alpha_3) = (59°,\, 244°,\, 91°)$; $\lambda \simeq 0.05$ ($M_1 \simeq 10^{11.6}\,\text{GeV}$) for BMPcI and $(\delta,\, \alpha_2,\, \alpha_3) = (301°,\, 116°,\, 269°)$. For Set II, we find: $\lambda \simeq 0.305$ ($M_1 \simeq 10^{12.8}\,\text{GeV}$) for BMPa and $(\delta,\, \alpha_2,\, \alpha_3) = (132°,\, 135°,\, 290°)$; $\lambda \simeq 0.25$ ($M_1 \simeq 10^{12.3}\,\text{GeV}$) for BMPb and $(\delta,\, \alpha_2,\, \alpha_3) = (228°,\, 225°,\, 70°)$; $\lambda \simeq 0.03$ ($M_1 \simeq 10^{11.2}\,\text{GeV}$) for BMPcII and $(\delta,\, \alpha_2,\, \alpha_3) = (228°,\, 225°,\, 70°)$. Overall, we find that leptogenesis is viable for $M_1 \gtrsim 10^{11}\,\text{GeV}$ across the entire parameter space. Qualitatively similar results hold in the case of thermal initial abundances of the right-handed neutrinos. See appendix A for more details.

JHEP09(2023)079

5 Conclusions

In this work, we have studied thermal leptogenesis in the context of the minimal gauged $\mathrm{U}(1)_{L_\mu - L_\tau}$ model. Given the light neutrino squared mass differences and the PMNS mixing angles as input, the model predicts the values of the lightest neutrino mass m_1, as well as the PMNS phases δ, α_2, and α_3. The model remains with three free parameters, which we have identified as λ, θ, and ϕ according to the parameterisation of the Yukawa couplings as in eq. (2.8). We have then performed a numerical scan of the parameter space and searched for the allowed ranges of λ, θ and ϕ for which leptogenesis is viable in reproducing the observed value of the baryon asymmetry of the Universe. To fully account for the effects of the charged lepton and heavy neutrino flavours, we have solved numerically the sets of density matrix equations instead of the simpler Boltzmann equations, and took the decays of all three right-handed neutrinos into account. Noting that thermal leptogenesis proceeds in the strong wash-out regime in the entire parameter space of the model so that the effects of scatterings and different initial conditions are typically sub-leading, we have focused only on direct and inverse decays and on the case of vanishing initial right-handed neutrino abundances. To avoid the non-physical behaviour in the CP-asymmetry due to degeneracy in the right-handed neutrino mass spectrum, we have included the full-resummed Yukawa couplings and resonant effects in the calculation, even though we found those to be relevant only in secluded regions of the parameter space.

We have found numerous regions in the parameter space where thermal leptogenesis within the minimal gauged $\mathrm{U}(1)_{L_\mu - L_\tau}$ model predicts the correct baryon asymmetry of the Universe. This result was not obvious given the restrictions in the neutrino mass structure imposed by the model. The size of the allowed regions for successful leptogenesis in the $\phi - \theta$ plane decreases with the mass scale of leptogenesis, which goes as λ^2, implying minimal values of the mass scale and λ for which leptogenesis can be successful. We found that thermal leptogenesis is viable for $M_1 \gtrsim 10^{11\text{–}12}\,\mathrm{GeV}$ across the entire parameter space, with λ taking values from order unity down to $\mathcal{O}(0.03\text{–}0.05)$. These values are larger than those obtained in the context of non-thermal leptogenesis within the minimal gauged $\mathrm{U}(1)_{L_\mu - L_\tau}$ model [24]. The difference is mostly due to the wash-out effects that are present in the thermal leptogenesis mechanism but not in the non-thermal scenario, implying relatively heavier right-handed neutrinos to satisfy the out-of-equilibrium condition.

The sign of the baryon asymmetry can be either positive or negative in the various regions, but leptogenesis is successful only where the baryon asymmetry is positive. However, after specifying the neutrino squared mass differences and the PMNS mixing angles, the minimal gauged $\mathrm{U}(1)_{L_\mu - L_\tau}$ model predicts two distinct sets of PMNS phases, $(\delta, \alpha_2, \alpha_3)$ and $(2\pi - \delta, 2\pi - \alpha_2, 2\pi - \alpha_3)$, each corresponding to opposite signs of the predicted baryon asymmetry. At present, the uncertainty on the estimate of δ obtained in the global analysis [57] is relatively large so that, in general, both predictions are plausible (to a certain level of confidence). We are then allowed to change the sign of the predicted asymmetry by switching from one set of PMNS phases to the other. The baryon asymmetry also has an opposite sign depending on whether θ_{23} lies above or below $\pi/4$. According to the 3σ ranges for θ_{23} obtained in the global analysis [57], see table 2, both cases are still valid,

JHEP09(2023)079

and it is, therefore, impossible to discriminate the sign of the baryon asymmetry in a given region of the parameter space. Of course, with future more accurate measurements of the Dirac phase δ and of the mixing angle θ_{23} from, e.g., T2K [97], NOνA [98], DUNE [99], and Hyper-Kamiokande [100] (see also ref. [101]), we would be able to rule out the certain region of the parameter space of leptogenesis in the considered model only on the basis of the sign of the baryon asymmetry. We stress that the results of this work are obtained for two different extreme choices of θ_{23} corresponding to the $\pm 3\sigma$ limit values of the global analysis, so to minimize the sum of neutrino masses, $\sum_i m_i$, and the tension with the cosmological bounds. In the future, more precise measurements of θ_{23} and/or $\sum_i m_i$ will likely impose even more stringent constraints on the model presented here.

Acknowledgments

A.G. wishes to thank the Kavli IPMU and the Department of Physics of the University of Tokyo at Hongo Campus for the kind hospitality offered during the first part of this project. A.G. acknowledges the use of computational resources from the parallel computing cluster of the Open Physics Hub (https://site.unibo.it/openphysicshub/en) at the Physics and Astronomy Department in Bologna. The work of A.G. has received funding from the European Union's Horizon Europe research and innovation programme under the Marie Skłodowska-Curie Staff Exchange grant agreement No. 101086085 — ASYMMETRY. The work of K.H., N.N., and M.R.Q. was supported in part by the Grant-in-Aid for Innovative Areas (No. 19H05810 [K.H.], No. 19H05802 [K.H.], No. 18H05542 [N.N.]), Scientific Research B (No. 20H01897 [K.H., N.N., and M.R.Q.]), and Young Scientists (No. 21K13916 [N.N.]). The work of J.W. is supported by the JSPS KAKENHI Grant (No. 22J21260).

A The case of thermal initial abundance

We show in figure 4 the results of the parameter scan in the case of right-handed neutrino thermal initial abundances, i.e., $N_{N_j}(z_{\rm in}) = N^{\rm eq}_{N_j}(0) = 3/4$, $j = 1, 2, 3$. The plots in the figure reveal some differences with respect to the vanishing initial abundance case in figure 2, indicating a dependence on the initial conditions in the scenario considered in this work. The differences, however, appear for larger values of λ and concentrate in the outer part of the $\phi - \theta$ plane. In these regions, given the parametrisation of the Yukawa couplings in eq. (2.8), we can have that one of the flavour is weakly coupled with either $\lambda_{e,\mu,\tau} \ll \lambda$, avoiding the wash-outs processes even if the overall strong regime holds, i.e., $\kappa_{1,2,3} \gg 1$. As λ takes smaller values, the regions of viable leptogenesis reduce in size and concentrate in the inner regions of the parameter space. For $\lambda = 0.3$, the regions are more similar to those obtained in the vanishing initial abundance case, with no prominent dependence on the initial conditions. This means that, in terms of allowed ranges of masses and couplings, we obtain qualitatively similar results as in the vanishing initial abundance case.

JHEP09(2023)079

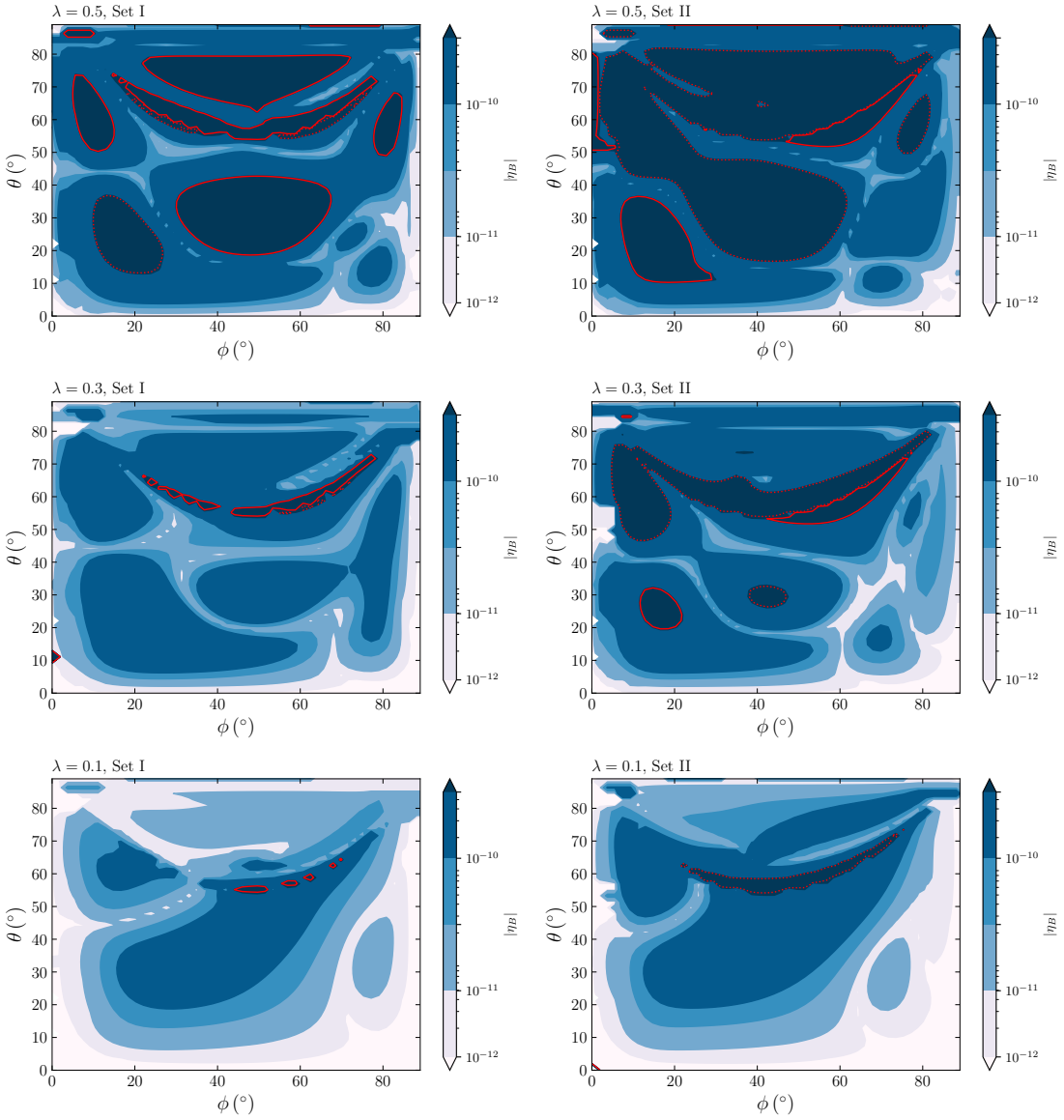

Figure 4. The contour plots in the $\phi - \theta$ plane of the BAU (in modulus) predicted by the DMEs with three decaying right-handed neutrinos in the case of thermal initial abundance. The details of the plots are as in figure 2.

B The impact of resonance effects

In this appendix, we estimate the relevance of the resonance effects of the CP-asymmetry in our numerical analysis. We first note that $\Delta M_{kj}/\Gamma_j \propto \lambda^{-2}$ meaning that, for a given point in the $\phi - \theta$ plane, the resonance effects are depleted if λ is sufficiently small. We show in figure 5 the points of our scan for which we find that $\Delta M_{21}/\Gamma_1 \lesssim 10$ (left panel) and $\Delta M_{32}/\Gamma_2 \lesssim 10$ (right panel) for $\lambda = 1$ (top panels) and 0.5 (bottom panels). The figure is obtained for the neutrino mixing angles and squared mass differences as in Set I. The results remain qualitatively similar for the input parameters in Set II and are thus not

JHEP09(2023)079

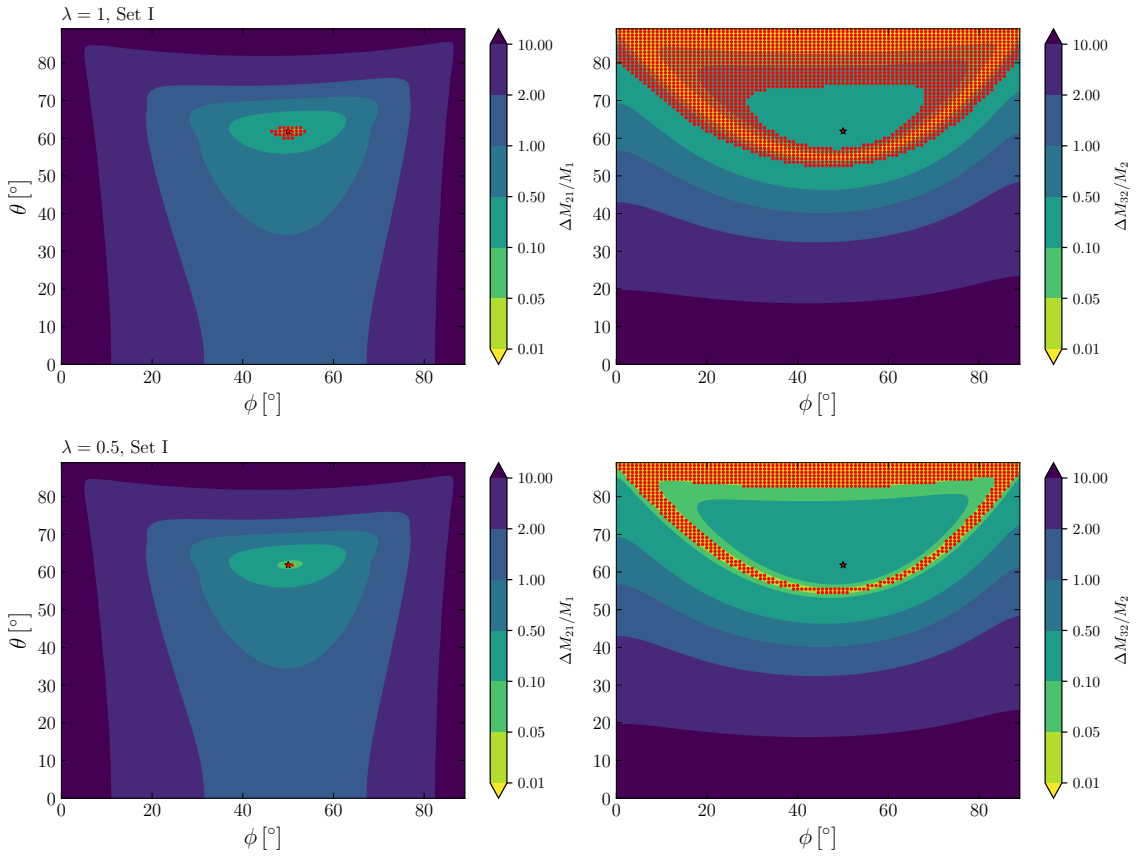

Figure 5. The red points in the left and right panels are those for which we find $\Delta M_{21}/\Gamma_1 \lesssim 10$ and $\Delta M_{32}/\Gamma_2 \lesssim 10$, respectively. The points in the top (bottom) panels are obtained for $\lambda = 1\,(0.5)$. The figure is obtained for the input parameters as in Set I. The remaining details of the plots are as in the bottom panels of figure 1.

shown here. The plots in the top panels show that, when $\lambda = 1$, we have $\Delta M_{21}/\Gamma_1 \lesssim 10$ and $\Delta M_{32}/\Gamma_2 \lesssim 10$ in the region of the parameter space corresponding to $M_2 \lesssim 1.5M_1$ and $M_3 \lesssim 1.5M_2$, respectively. When $\lambda = 0.5$, these regions are reduced, and it becomes difficult to find points satisfying the two inequalities for $\lambda < 0.5$. This indicates that resonance effects are negligible in most of the parameter space when $\lambda \lesssim 0.5$. By comparing the plots in the left and right panels, it follows that there is no region where the three right-handed neutrinos are simultaneously in the resonant regime, thus justifying the use of the regularisation in eq. (3.8) in the main analysis.

JHEP09(2023)079

References

[1] Planck collaboration, *Planck 2018 results. VI. Cosmological parameters*, *Astron. Astrophys.* **641** (2020) A6 [*Erratum ibid.* **652** (2021) C4] [arXiv:1807.06209] [INSPIRE].

[2] R.J. Cooke, M. Pettini and C.C. Steidel, *One Percent Determination of the Primordial Deuterium Abundance*, *Astrophys. J.* **855** (2018) 102 [arXiv:1710.11129] [INSPIRE].

[3] M. Fukugita and T. Yanagida, *Baryogenesis Without Grand Unification*, *Phys. Lett. B* **174** (1986) 45 [INSPIRE].

[4] V.A. Kuzmin, V.A. Rubakov and M.E. Shaposhnikov, *On the Anomalous Electroweak Baryon Number Nonconservation in the Early Universe*, *Phys. Lett. B* **155** (1985) 36 [INSPIRE].

[5] D. Bodeker and W. Buchmüller, *Baryogenesis from the weak scale to the grand unification scale*, *Rev. Mod. Phys.* **93** (2021) 035004 [arXiv:2009.07294] [INSPIRE].

[6] R. Foot, *New Physics From Electric Charge Quantization?*, *Mod. Phys. Lett. A* **6** (1991) 527 [INSPIRE].

[7] X.G. He, G.C. Joshi, H. Lew and R.R. Volkas, *New Z' phenomenology*, *Phys. Rev. D* **43** (1991) 22 [INSPIRE].

[8] X.-G. He, G.C. Joshi, H. Lew and R.R. Volkas, *Simplest Z' model*, *Phys. Rev. D* **44** (1991) 2118 [INSPIRE].

[9] R. Foot, X.G. He, H. Lew and R.R. Volkas, *Model for a light Z' boson*, *Phys. Rev. D* **50** (1994) 4571 [hep-ph/9401250] [INSPIRE].

[10] P. Minkowski, $\mu \to e\gamma$ *at a Rate of One Out of* 10^9 *Muon Decays?*, *Phys. Lett. B* **67** (1977) 421 [INSPIRE].

[11] T. Yanagida, *Horizontal gauge symmetry and masses of neutrinos*, *Conf. Proc. C* **7902131** (1979) 95 [INSPIRE].

[12] M. Gell-Mann, P. Ramond and R. Slansky, *Complex Spinors and Unified Theories*, *Conf. Proc. C* **790927** (1979) 315 [arXiv:1306.4669] [INSPIRE].

[13] S.L. Glashow, *The Future of Elementary Particle Physics*, *NATO Sci. Ser. B* **61** (1980) 687 [INSPIRE].

[14] R.N. Mohapatra and G. Senjanovic, *Neutrino Mass and Spontaneous Parity Nonconservation*, *Phys. Rev. Lett.* **44** (1980) 912 [INSPIRE].

[15] G.C. Branco, W. Grimus and L. Lavoura, *The Seesaw Mechanism in the Presence of a Conserved Lepton Number*, *Nucl. Phys. B* **312** (1989) 492 [INSPIRE].

[16] S. Choubey and W. Rodejohann, *A Flavor symmetry for quasi-degenerate neutrinos: $L_\mu - L_\tau$*, *Eur. Phys. J. C* **40** (2005) 259 [hep-ph/0411190] [INSPIRE].

[17] T. Araki, J. Heeck and J. Kubo, *Vanishing Minors in the Neutrino Mass Matrix from Abelian Gauge Symmetries*, *JHEP* **07** (2012) 083 [arXiv:1203.4951] [INSPIRE].

[18] J. Heeck, *Neutrinos and Abelian Gauge Symmetries*, Ph.D. Thesis, Heidelberg U. (2014) [INSPIRE].

[19] A. Crivellin, G. D'Ambrosio and J. Heeck, *Addressing the LHC flavor anomalies with horizontal gauge symmetries*, *Phys. Rev. D* **91** (2015) 075006 [arXiv:1503.03477] [INSPIRE].

[20] R. Plestid, *Consequences of an Abelian Z' for neutrino oscillations and dark matter*, *Phys. Rev. D* **93** (2016) 035011 [arXiv:1602.06651] [INSPIRE].

JHEP09(2023)079

[21] K. Asai, K. Hamaguchi and N. Nagata, *Predictions for the neutrino parameters in the minimal gauged* $\mathrm{U}(1)_{L_\mu - L_\tau}$ *model*, *Eur. Phys. J. C* **77** (2017) 763 [arXiv:1705.00419] [INSPIRE].

[22] K. Asai et al., *Minimal Gauged* $\mathrm{U}(1)_{L_\alpha - L_\beta}$ *Models Driven into a Corner*, *Phys. Rev. D* **99** (2019) 055029 [arXiv:1811.07571] [INSPIRE].

[23] K. Asai, *Predictions for the neutrino parameters in the minimal model extended by linear combination of* $\mathrm{U}(1)_{L_e - L_\mu}$, $\mathrm{U}(1)_{L_\mu - L_\tau}$ *and* $\mathrm{U}(1)_{B-L}$ *gauge symmetries*, *Eur. Phys. J. C* **80** (2020) 76 [arXiv:1907.04042] [INSPIRE].

[24] K. Asai, K. Hamaguchi, N. Nagata and S.-Y. Tseng, *Leptogenesis in the minimal gauged* $\mathrm{U}(1)_{L_\mu - L_\tau}$ *model and the sign of the cosmological baryon asymmetry*, *JCAP* **11** (2020) 013 [arXiv:2005.01039] [INSPIRE].

[25] D. Borah, A. Dasgupta and D. Mahanta, *TeV scale resonant leptogenesis with* $L_\mu - L_\tau$ *gauge symmetry in light of the muon g-2*, *Phys. Rev. D* **104** (2021) 075006 [arXiv:2106.14410] [INSPIRE].

[26] X.X. Qi, W. Liu and H. Sun, *Leptogenesis and light scalar dark matter in a* $L_\mu - L_\tau$ *model*, arXiv:2204.01086 [INSPIRE].

[27] S. Eijima, M. Ibe and K. Murai, *Muon* $g-2$ *and non-thermal leptogenesis in* $\mathrm{U}(1)_{L_\mu - L_\tau}$ *model*, *JHEP* **05** (2023) 010 [arXiv:2303.09751] [INSPIRE].

[28] S. Blanchet and P. Di Bari, *The minimal scenario of leptogenesis*, *New J. Phys.* **14** (2012) 125012 [arXiv:1211.0512] [INSPIRE].

[29] S. Davidson and A. Ibarra, *A Lower bound on the right-handed neutrino mass from leptogenesis*, *Phys. Lett. B* **535** (2002) 25 [hep-ph/0202239] [INSPIRE].

[30] W. Buchmüller, P. Di Bari and M. Plümacher, *Cosmic microwave background, matter-antimatter asymmetry and neutrino masses*, *Nucl. Phys. B* **643** (2002) 367 [*Erratum ibid.* **793** (2008) 362] [hep-ph/0205349] [INSPIRE].

[31] J.R. Ellis and M. Raidal, *Leptogenesis and the violation of lepton number and CP at low-energies*, *Nucl. Phys. B* **643** (2002) 229 [hep-ph/0206174] [INSPIRE].

[32] W. Buchmüller, P. Di Bari and M. Plümacher, *The Neutrino mass window for baryogenesis*, *Nucl. Phys. B* **665** (2003) 445 [hep-ph/0302092] [INSPIRE].

[33] W. Buchmüller, P. Di Bari and M. Plümacher, *Leptogenesis for pedestrians*, *Annals Phys.* **315** (2005) 305 [hep-ph/0401240] [INSPIRE].

[34] R. Barbieri, P. Creminelli, A. Strumia and N. Tetradis, *Baryogenesis through leptogenesis*, *Nucl. Phys. B* **575** (2000) 61 [hep-ph/9911315] [INSPIRE].

[35] H.B. Nielsen and Y. Takanishi, *Baryogenesis via lepton number violation and family replicated gauge group*, *Nucl. Phys. B* **636** (2002) 305 [hep-ph/0204027] [INSPIRE].

[36] T. Endoh, T. Morozumi and Z.-H. Xiong, *Primordial lepton family asymmetries in seesaw model*, *Prog. Theor. Phys.* **111** (2004) 123 [hep-ph/0308276] [INSPIRE].

[37] E. Nardi, Y. Nir, E. Roulet and J. Racker, *The Importance of flavor in leptogenesis*, *JHEP* **01** (2006) 164 [hep-ph/0601084] [INSPIRE].

[38] A. Abada et al., *Flavor issues in leptogenesis*, *JCAP* **04** (2006) 004 [hep-ph/0601083] [INSPIRE].

JHEP09(2023)079

[39] A. Abada et al., *Flavour Matters in Leptogenesis*, *JHEP* **09** (2006) 010 [hep-ph/0605281] [INSPIRE].

[40] A. De Simone and A. Riotto, *On the impact of flavour oscillations in leptogenesis*, *JCAP* **02** (2007) 005 [hep-ph/0611357] [INSPIRE].

[41] S. Blanchet, P. Di Bari and G.G. Raffelt, *Quantum Zeno effect and the impact of flavor in leptogenesis*, *JCAP* **03** (2007) 012 [hep-ph/0611337] [INSPIRE].

[42] S. Blanchet, P. Di Bari, D.A. Jones and L. Marzola, *Leptogenesis with heavy neutrino flavours: from density matrix to Boltzmann equations*, *JCAP* **01** (2013) 041 [arXiv:1112.4528] [INSPIRE].

[43] P.S.B. Dev et al., *Flavor effects in leptogenesis*, *Int. J. Mod. Phys. A* **33** (2018) 1842001 [arXiv:1711.02861] [INSPIRE].

[44] K. Moffat et al., *Three-flavored nonresonant leptogenesis at intermediate scales*, *Phys. Rev. D* **98** (2018) 015036 [arXiv:1804.05066] [INSPIRE].

[45] A. Granelli, K. Moffat and S.T. Petcov, *Aspects of high scale leptogenesis with low-energy leptonic CP violation*, *JHEP* **11** (2021) 149 [arXiv:2107.02079] [INSPIRE].

[46] A. Granelli et al., *ULYSSES: Universal LeptogeneSiS Equation Solver*, *Comput. Phys. Commun.* **262** (2021) 107813 [arXiv:2007.09150] [INSPIRE].

[47] A. Granelli et al., *ULYSSES, universal LeptogeneSiS equation solver: Version 2*, *Comput. Phys. Commun.* **291** (2023) 108834 [arXiv:2301.05722] [INSPIRE].

[48] H.K. Dreiner, H.E. Haber and S.P. Martin, *Two-component spinor techniques and Feynman rules for quantum field theory and supersymmetry*, *Phys. Rept.* **494** (2010) 1 [arXiv:0812.1594] [INSPIRE].

[49] L. Lavoura, *Zeros of the inverted neutrino mass matrix*, *Phys. Lett. B* **609** (2005) 317 [hep-ph/0411232] [INSPIRE].

[50] E.I. Lashin and N. Chamoun, *Zero minors of the neutrino mass matrix*, *Phys. Rev. D* **78** (2008) 073002 [arXiv:0708.2423] [INSPIRE].

[51] B. Pontecorvo, *Neutrino Experiments and the Problem of Conservation of Leptonic Charge*, *Zh. Eksp. Teor. Fiz.* **53** (1967) 1717 [INSPIRE].

[52] B. Pontecorvo, *Mesonium and anti-mesonium*, *Sov. Phys. JETP* **6** (1957) 429 [INSPIRE].

[53] B. Pontecorvo, *Inverse beta processes and nonconservation of lepton charge*, *Zh. Eksp. Teor. Fiz.* **34** (1957) 247 [INSPIRE].

[54] Z. Maki, M. Nakagawa and S. Sakata, *Remarks on the unified model of elementary particles*, *Prog. Theor. Phys.* **28** (1962) 870 [INSPIRE].

[55] Particle Data Group collaboration, *Review of Particle Physics*, *Phys. Rev. D* **98** (2018) 030001 [INSPIRE].

[56] NuFIT collaboration, *NuFIT v5.2*, http://www.nu-fit.org.

[57] I. Esteban et al., *The fate of hints: updated global analysis of three-flavor neutrino oscillations*, *JHEP* **09** (2020) 178 [arXiv:2007.14792] [INSPIRE].

[58] Particle Data Group collaboration, *Review of Particle Physics*, *PTEP* **2020** (2020) 083C01 [INSPIRE].

JHEP09(2023)079

[59] F. Capozzi et al., *Global constraints on absolute neutrino masses and their ordering*, *Phys. Rev. D* **95** (2017) 096014 [*Addendum ibid.* **101** (2020) 116013] [arXiv:2003.08511] [INSPIRE].

[60] S. Vagnozzi et al., *Unveiling ν secrets with cosmological data: neutrino masses and mass hierarchy*, *Phys. Rev. D* **96** (2017) 123503 [arXiv:1701.08172] [INSPIRE].

[61] S. Roy Choudhury and S. Hannestad, *Updated results on neutrino mass and mass hierarchy from cosmology with Planck 2018 likelihoods*, *JCAP* **07** (2020) 037 [arXiv:1907.12598] [INSPIRE].

[62] M.M. Ivanov, M. Simonović and M. Zaldarriaga, *Cosmological Parameters and Neutrino Masses from the Final Planck and Full-Shape BOSS Data*, *Phys. Rev. D* **101** (2020) 083504 [arXiv:1912.08208] [INSPIRE].

[63] DES collaboration, *Dark Energy Survey Year 3 results: Cosmological constraints from galaxy clustering and weak lensing*, *Phys. Rev. D* **105** (2022) 023520 [arXiv:2105.13549] [INSPIRE].

[64] I. Tanseri et al., *Updated neutrino mass constraints from galaxy clustering and CMB lensing-galaxy cross-correlation measurements*, *JHEAp* **36** (2022) 1 [arXiv:2207.01913] [INSPIRE].

[65] KamLAND-Zen collaboration, *Search for the Majorana Nature of Neutrinos in the Inverted Mass Ordering Region with KamLAND-Zen*, *Phys. Rev. Lett.* **130** (2023) 051801 [arXiv:2203.02139] [INSPIRE].

[66] M. Agostini, G. Benato and J. Detwiler, *Discovery probability of next-generation neutrinoless double-β decay experiments*, *Phys. Rev. D* **96** (2017) 053001 [arXiv:1705.02996] [INSPIRE].

[67] C. Adams et al., *Neutrinoless Double Beta Decay*, arXiv:2212.11099 [INSPIRE].

[68] K. Moffat, S. Pascoli, S.T. Petcov and J. Turner, *Leptogenesis from Low Energy CP Violation*, *JHEP* **03** (2019) 034 [arXiv:1809.08251] [INSPIRE].

[69] A. Granelli, K. Moffat and S.T. Petcov, *Flavoured resonant leptogenesis at sub-TeV scales*, *Nucl. Phys. B* **973** (2021) 115597 [arXiv:2009.03166] [INSPIRE].

[70] F. Hahn-Woernle, M. Plümacher and Y.Y.Y. Wong, *Full Boltzmann equations for leptogenesis including scattering*, *JCAP* **08** (2009) 028 [arXiv:0907.0205] [INSPIRE].

[71] S. Blanchet and P. Di Bari, *Flavor effects on leptogenesis predictions*, *JCAP* **03** (2007) 018 [hep-ph/0607330] [INSPIRE].

[72] B. Garbrecht, *More Viable Parameter Space for Leptogenesis*, *Phys. Rev. D* **90** (2014) 063522 [arXiv:1401.3278] [INSPIRE].

[73] T. Frossard, A. Kartavtsev and D. Mitrouskas, *Systematic approach to $\Delta L = 1$ processes in thermal leptogenesis*, *Phys. Rev. D* **87** (2013) 125006 [arXiv:1304.1719] [INSPIRE].

[74] B. Garbrecht, P. Klose and C. Tamarit, *Relativistic and spectator effects in leptogenesis with heavy sterile neutrinos*, *JHEP* **02** (2020) 117 [arXiv:1904.09956] [INSPIRE].

[75] M. Flanz, E.A. Paschos and U. Sarkar, *Baryogenesis from a lepton asymmetric universe*, *Phys. Lett. B* **345** (1995) 248 [*Erratum ibid.* **382** (1996) 447] [*Erratum ibid.* **384** (1996) 487] [hep-ph/9411366] [INSPIRE].

[76] L. Covi, E. Roulet and F. Vissani, *CP violating decays in leptogenesis scenarios*, *Phys. Lett. B* **384** (1996) 169 [hep-ph/9605319] [INSPIRE].

JHEP09(2023)079

[77] L. Covi and E. Roulet, *Baryogenesis from mixed particle decays*, *Phys. Lett. B* **399** (1997) 113 [hep-ph/9611425] [INSPIRE].

[78] W. Buchmüller and M. Plümacher, *CP asymmetry in Majorana neutrino decays*, *Phys. Lett. B* **431** (1998) 354 [hep-ph/9710460] [INSPIRE].

[79] S. Biondini et al., *Status of rates and rate equations for thermal leptogenesis*, *Int. J. Mod. Phys. A* **33** (2018) 1842004 [arXiv:1711.02864] [INSPIRE].

[80] A. Pilaftsis, *CP violation and baryogenesis due to heavy Majorana neutrinos*, *Phys. Rev. D* **56** (1997) 5431 [hep-ph/9707235] [INSPIRE].

[81] A. Pilaftsis, *Resonant CP violation induced by particle mixing in transition amplitudes*, *Nucl. Phys. B* **504** (1997) 61 [hep-ph/9702393] [INSPIRE].

[82] A. Pilaftsis and T.E.J. Underwood, *Resonant leptogenesis*, *Nucl. Phys. B* **692** (2004) 303 [hep-ph/0309342] [INSPIRE].

[83] A. Pilaftsis and T.E.J. Underwood, *Electroweak-scale resonant leptogenesis*, *Phys. Rev. D* **72** (2005) 113001 [hep-ph/0506107] [INSPIRE].

[84] T. Hambye, *Leptogenesis at the TeV scale*, *Nucl. Phys. B* **633** (2002) 171 [hep-ph/0111089] [INSPIRE].

[85] T. Hambye, J. March-Russell and S.M. West, *TeV scale resonant leptogenesis from supersymmetry breaking*, *JHEP* **07** (2004) 070 [hep-ph/0403183] [INSPIRE].

[86] V. Cirigliano, G. Isidori and V. Porretti, *CP violation and Leptogenesis in models with Minimal Lepton Flavour Violation*, *Nucl. Phys. B* **763** (2007) 228 [hep-ph/0607068] [INSPIRE].

[87] Z.-Z. Xing and S. Zhou, *Tri-bimaximal Neutrino Mixing and Flavor-dependent Resonant Leptogenesis*, *Phys. Lett. B* **653** (2007) 278 [hep-ph/0607302] [INSPIRE].

[88] G.C. Branco et al., *Another look at minimal lepton flavour violation, $l_i \to l_{j\gamma}$, leptogenesis, and the ratio M_ν/Λ_{LFV}*, *JHEP* **09** (2007) 004 [hep-ph/0609067] [INSPIRE].

[89] E.J. Chun and K. Turzynski, *Quasi-degenerate neutrinos and leptogenesis from $L_\mu - L_\tau$*, *Phys. Rev. D* **76** (2007) 053008 [hep-ph/0703070] [INSPIRE].

[90] T. Kitabayashi, *Remark on the minimal seesaw model and leptogenesis with tri/bi-maximal mixing*, *Phys. Rev. D* **76** (2007) 033002 [hep-ph/0703303] [INSPIRE].

[91] F.F. Deppisch, P.S. Bhupal Dev and A. Pilaftsis, *Neutrinos and Collider Physics*, *New J. Phys.* **17** (2015) 075019 [arXiv:1502.06541] [INSPIRE].

[92] I. Brivio et al., *Leptogenesis in the Neutrino Option*, *JHEP* **10** (2019) 059 [*Erratum ibid.* **02** (2020) 148] [arXiv:1905.12642] [INSPIRE].

[93] B. Dev et al., *Resonant enhancement in leptogenesis*, *Int. J. Mod. Phys. A* **33** (2018) 1842003 [arXiv:1711.02863] [INSPIRE].

[94] M. Garny, A. Kartavtsev and A. Hohenegger, *Leptogenesis from first principles in the resonant regime*, *Annals Phys.* **328** (2013) 26 [arXiv:1112.6428] [INSPIRE].

[95] P.S. Bhupal Dev, P. Millington, A. Pilaftsis and D. Teresi, *Flavour effects in Resonant Leptogenesis from semi-classical and Kadanoff-Baym approaches*, *J. Phys. Conf. Ser.* **631** (2015) 012087 [arXiv:1502.07987] [INSPIRE].

JHEP09(2023)079

[96] P.C. da Silva, D. Karamitros, T. McKelvey and A. Pilaftsis, *Tri-Resonant Leptogenesis*, arXiv:2303.15227 [INSPIRE].

[97] T2K collaboration, *The T2K Experiment*, *Nucl. Instrum. Meth. A* **659** (2011) 106 [arXiv:1106.1238] [INSPIRE].

[98] NOvA collaboration, *Improved measurement of neutrino oscillation parameters by the NOvA experiment*, *Phys. Rev. D* **106** (2022) 032004 [arXiv:2108.08219] [INSPIRE].

[99] DUNE collaboration, *Deep Underground Neutrino Experiment (DUNE) Near Detector Conceptual Design Report*, *Instruments* **5** (2021) 31 [arXiv:2103.13910] [INSPIRE].

[100] HYPER-KAMIOKANDE collaboration, *Hyper-Kamiokande Experiment: A Snowmass White Paper*, in the proceedings of the *Snowmass 2021*, (2022) [arXiv:2203.02029] [INSPIRE].

[101] P. Huber et al., *Snowmass Neutrino Frontier Report*, in the proceedings of the *Snowmass 2021*, (2022) [arXiv:2211.08641] [INSPIRE].

JHEP09(2023)079